Chemical Biology & Drug Design

WILEY

RESEARCH ARTICLE OPEN ACCESS

Synthesis of Novel Thiazole/Thiadiazole Conjugates of Fluoroquinolones as Potent Antibacterial and Antimycobacterial Agents

Pınar Poyraz Yılmaz[1] | Necla Kulabaş[2] | Arif Bozdeveci[3] | Siva Krishna Vagolu[4,5] | Mohd Imran[6] | Esra Tatar[2,7] | Şengül Alpay Karaoğlu[3] | Dharmarajan Sriram[8] | Ammar A. Razzak Mahmood[9] | İlkay Küçükgüzel[1,10]

[1]Institute of Health Sciences, Marmara University, İstanbul, Turkey | [2]Department of Pharmaceutical Chemistry, Faculty of Pharmacy, Marmara University, İstanbul, Turkey | [3]Department of Biology, Faculty of Arts and Sciences, Recep Tayyip Erdoğan University, Rize, Turkey | [4]Department of Microbiology, University of Oslo, Oslo, Norway | [5]Research Institute of Internal Medicine, Oslo University Hospital, Oslo, Norway | [6]Center for Health Research, Northern Border University, Arar, Saudi Arabia | [7]Department of Pharmaceutical Chemistry, Faculty of Pharmacy, İstanbul Kent University, İstanbul, Turkey | [8]Department of Pharmacy, Birla Institute of Technology & Science-Pilani, Hyderabad Campus, Hyderabad, India | [9]Department of Pharmaceutical Chemistry, College of Pharmacy, University of Baghdad, Baghdad, Iraq | [10]Department of Pharmaceutical Chemistry, Faculty of Pharmacy, Fenerbahçe University, İstanbul, Turkey

Correspondence: İlkay Küçükgüzel (ilkay.kucukguzel@fbu.edu.tr)

Received: 30 April 2025 | **Revised:** 30 April 2025 | **Accepted:** 11 May 2025

Funding: This work was supported by Marmara Üniversitesi, SAG-C-DRP-140115-0002.

Keywords: antibacterial activity | antituberculosis activity | DNA-gyrase | fluoroquinolones | molecular docking

ABSTRACT

Twenty azole-fluoroquinolone hybrids were designed and synthesized by conjugating thiazole and thiadiazole structures to ciprofloxacin and norfloxacin via a 2-oxoethyl bridge. The structures and purities of the synthesized compounds were proven by spectral techniques. The antimycobacterial effects of target compounds **21–40** were tested against *Mycobacterium tuberculosis* H37Rv strain. Among the 20 synthesized compounds, 12 exhibited minimal inhibition concentration (MIC) values in the range of 1.56–25 μg/mL. Among the molecules screened for antimycobacterial effects, the most effective was compound **35**, a thiadiazole-ciprofloxacin hybrid. The cytotoxic effect of this molecule was found to be lower than the reference drugs, and it was also determined to be a more effective inhibitor than ciprofloxacin and norfloxacin in the DNA-gyrase supercoiling test. The antimicrobial effects of compounds **21–40** were screened by agar-well diffusion and microdilution tests against Gram-positive/negative bacteria, a fast-growing mycobacterium, and two yeast strains. While most of the compounds tested showed antibacterial effects, the most effective fluoroquinolone derivative appeared to be compound **31** with an MIC value of <0.63 μg/mL against all Gram-negative bacteria tested. Azole-fluoroquinolone hybrids **21–40** did not show any activity against non-pathogenic *Lactobacillus* species and yeast-like fungi, indicating that they have selective antibacterial and antimycobacterial activity, particularly against Gram-negative bacteria. *In silico* molecular docking studies were conducted to uncover the interactions between lead compound **35** and the DNA gyrase proteins of *M. tuberculosis* and *S. aureus*. Additionally, a 100 ns molecular dynamics simulation was carried out to assess the stability of the complexes formed between compound **35** and both proteins.

This research was partly presented at the 2nd International Gazi Pharma Symposium Series (GPSS 2017) on 11-13 October 2017, Ankara, Türkiye.

1 | Introduction

The fluoroquinolones (FQs) are currently among the most commonly used antimicrobials for treating bacterial infections due to their broad-spectrum activity, good penetration, and favorable safety profiles (Nishida et al. 2017). Quinolones are broad-spectrum antibacterial drugs that directly inhibit DNA synthesis. The history of quinolones began with the discovery of 3-carboxy substituted quinolones in 1949 (Bisacchi 2015). Quinolones are classified into four generations based on their antibacterial spectrum. Nalidixic acid belongs to the first-generation quinolone class and entered clinical use in 1962 (Lesher et al. 1962). Nalidixic acid has been reported to be insufficient in the treatment of systemic infections due to its very polar nature and high binding to serum proteins. However, since both nalidixic acid and its active 7-hydroxymethyl metabolite are subject to rapid renal excretion and accumulate easily in the urinary tract, new derivatives were designed to overcome these problems (Heeb et al. 2011). In the following years, second-generation quinolone derivatives called fluoroquinolones entered the treatment. Fluoroquinolones were effective against both Gram-positive and Gram-negative bacteria, thereby broadening their spectrum of action and improving their pharmacokinetic properties compared to first-generation derivatives.

Norfloxacin, the first representative of fluoroquinolones developed for use in the treatment of renal and abdominal infections, respiratory system infections, and sexually transmitted bacterial infections, was synthesized in 1978 and entered clinical use in 1986 (Heeb et al. 2011; Paton et al. 1988). Another second-generation drug is ciprofloxacin, which was introduced to the market in 1987 and is one of the most widely used fluoroquinolones. Third-generation drugs were developed to create more potent fluoroquinolones. The piperazinyl substituent at the 7th position of the quinolone ring is usually conserved. However, new compounds may also include derivatives with a pyrrolidinyl moiety instead. Levofloxacin, one of the most important drugs of the third-generation quinolones, was introduced into clinical practice in 1996. Levofloxacin shows broad-spectrum activity against Gram-positive and Gram-negative bacteria as well as atypical respiratory pathogens (Blondeau et al. 2004). In recent years, treatment regimens combining levofloxacin with amoxicillin and a proton pump inhibitor have been reported for the treatment of *Helicobacter pylori* infections (Chuah et al. 2011).

Due to the increasing resistance mechanisms against fluoroquinolones, new compounds have been developed to treat infections due to Gram-positive organisms, and fourth generation fluoroquinolones have emerged. Moxifloxacin, one of the most important members of this group, was introduced into clinical practice in 1999. Based on the chemical structure of ciprofloxacin and designed to impart activity against anaerobic pathogens, a methoxy substituent was added at position 8 of the moxifloxacin molecule (Blondeau et al. 2004).

Tuberculosis (TB) and its causative agent *Mycobacterium tuberculosis* present a serious threat to global health. Affecting all countries and age groups, TB infects an average of 10 million people each year. Despite being a preventable and treatable disease, tuberculosis remained the most common infectious disease worldwide in 2023, resulting in the deaths of 1.25 million people. It is the leading cause of mortality among individuals living with HIV and also plays a critical role in deaths linked to antimicrobial resistance (WHO 2024). The ideal strategy to such challenges is to discover novel agents that inhibit new targets in pathogens, but a more practical approach is to modify the structures of existing antibacterial agents to increase potency and to overcome resistance (Huang et al. 2016). Development of novel antibacterial agents with little or no bacterial resistance is therefore an important topic of current research (Panda et al. 2015).

The persistent emergence of multidrug-resistant (MDR) and extensively drug-resistant (XDR) tuberculosis strains poses a formidable challenge to global TB control strategies (Lange et al. 2019; Tiberi et al. 2022; WHO 2024). MDR-TB, characterized by resistance to at least isoniazid and rifampicin, and XDR-TB, exhibiting additional resistance to fluoroquinolones and second-line injectable agents such as amikacin, kanamycin, or capreomycin, severely restrict therapeutic options and complicate treatment regimens (Lange et al. 2019; Tiberi et al. 2022). This alarming trend underscores the imperative to identify and develop novel chemotherapeutic agents with distinct mechanisms of action capable of circumventing existing resistance profiles and enhancing treatment outcomes (Tiberi et al. 2022; WHO 2024).

Fluoroquinolones have been approved by the WHO as a second-line treatment agent in tuberculosis cases with multidrug resistance, and when used with first-line drugs, it has been reported that they reduce the number of colony-forming units more than first-line drugs (Sriram et al. 2006; Talath and Gadad 2006).

The emergence of isoniazid and rifampin-resistant tuberculosis cases in the early 1990s prompted clinicians to add ciprofloxacin to their treatment program, but resistance to ciprofloxacin was also found shortly thereafter. It has been reported that ofloxacin and levofloxacin have better pharmacokinetic properties and better penetration into macrophages than ciprofloxacin, resulting in improved treatment success. When it was determined that derivatives with a methoxy substituent in the 8th position of the quinolone ring were more effective against *M. tuberculosis* than other derivatives, cytafloxacin and sparfloxacin were introduced into tuberculosis treatment; however, both derivatives were reported to be phototoxic. Gatifloxacin used in the treatment of tuberculosis has also been reported to cause changes in glucose balance, especially in elderly patients. In recent years, most of the clinical studies on the use of fluoroquinolones for the treatment of tuberculosis have focused on moxifloxacin.

Quinolone antibiotics inhibit DNA synthesis by targeting two major type II topoisomerases: DNA gyrase (gyrase) and topoisomerase IV (topo IV) (Levine et al. 1998). As a result of genetic studies on mutant strains resistant to fluoroquinolones and studies with isolated topoisomerase enzymes, many of the antimicrobial fluoroquinolones show higher affinity for topoisomerase IV in Gram (+) bacteria such as *Staphylococcus aureus*, while they bind to DNA gyrase as the primary target in Gram

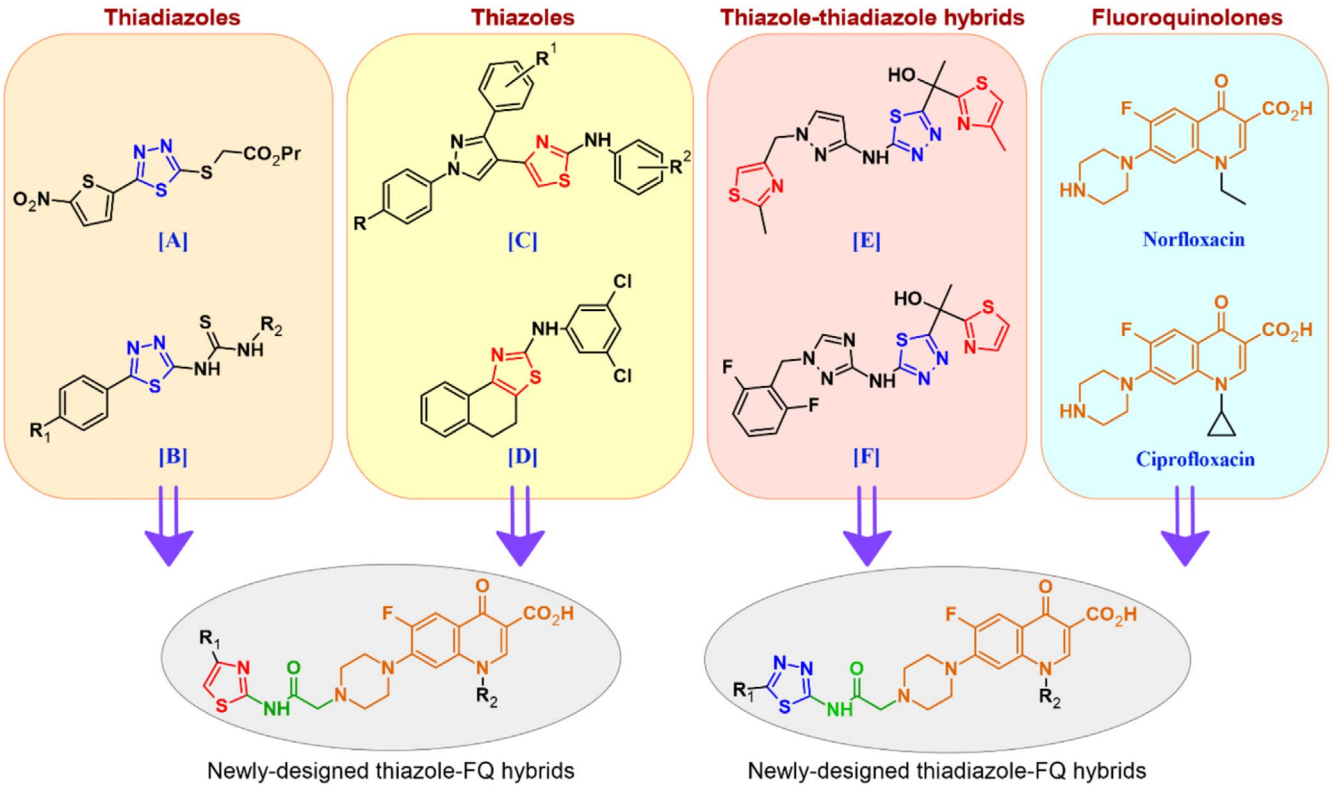

FIGURE 1 | Design strategy of new heterocylic conjugates of fluoroquinolones: (a) Isolation of thiazole/thiadiazole moiety from structures [**A**]–[**F**]; (b) attachment of the -**NH-CO-CH$_2$**- linker; (c) Hybridization with norfloxacin/ciprofloxacin.

(–) bacteria such as *Escherichia coli*. Compounds outside this rule have been reported to bind to both types of topoisomerase II (Nieto et al. 2005).

The ability of fluoroquinolones to potentially inhibit two different bacterial enzymes reduces the possibility of selecting resistant mutants (Wiles et al. 2010). Fluoroquinolones form a ternary complex with DNA and DNA gyrase (or topo IV) (fluoroquinolone–gyrase–DNA or fluoroquinolone–topoisomerase IV–DNA), thereby inhibiting replication and causing cell death (Froelich-ammon and Osheroff 1995).

Due to the widespread use (and overuse) of quinolones, the number of quinolone-resistant bacterial strains has been increasing steadily since the 1990s. As with other antibacterial agents, the increase in quinolone resistance threatens the clinical utility of this important class of drugs (Aldred et al. 2014). Resistance to these agents can result from various factors, including gene mutations, increased production of efflux pumps, modifying enzymes, or target-protection proteins. Quinolone resistance is mostly associated with specific mutations in gyrase and/or topoisomerase IV. Generally, a type II enzyme mutation confers $\leq$10 times more drug resistance (Anderson and Osheroff 2001; Drlica et al. 2009; Fournier et al. 2000; Hooper 1999, 2001; Price et al. 2003).

Thiadiazoles and thiazoles are heterocyclic rings whose antitubercular effects are frequently cited. Promising effects of thiadiazoles and their derivatives, alone or combined within the same molecule, against *M. tuberculosis* strains have been reported in previous studies. The antimycobacterial effects of 1,3,4-thiadiazole derivatives bearing thioether (compound **A**) or thiourea (compound **B**) side chains against *M. tuberculosis* H37Rv strain have been reported in previous studies (Foroumadi et al. 2006; Tatar et al. 2016). Thiazole compounds bearing arylamino residues (represented as compounds **C** and **D**) are also a heterocyclic group whose antitubercular effects have been investigated (Machado et al. 2018; Nandurkar et al. 2023). Of these, compound **D**, also known as UPAR-174, with the structure N-(3,5-dichlorophenyl)-4,5-dihydronaphtho[1,2-d][1,3]thiazol-2-amine, is effective against MDR *M. tuberculosis* strains; it also stands out with its feature that increases the effect of other drugs as an efflux inhibitor (Machado et al. 2018). Compound **E** (GSK-693) (Martínez-hoyos et al. 2016) and compound **F** (Shirude et al. 2013), which are methylthiazole-thiadiazole hybrids, have been reported in the literature as drug candidates due to their very low minimal inhibition concentration (MIC) values and nanomolar InhA inhibition.

Jazayeri et al., who designed thiadiazole-gatifloxacin hybrids, reported that these compounds showed strong antibacterial effects, especially against Gram-positive bacteria (Jazayeri et al. 2009). In our previous study, we conjugated 1,3,4-thiadiazole and fluoroquinolone structures and reported their antitubercular and antibacterial effects (Demirci et al. 2018). In our current study, 1,3,4-thiadiazole and thiazole conjugates were designed based on ciprofloxacin and norfloxacin (Figure 1). Our design strategy was to combine 2-amino-1,3,4-thiadiazole and 4-aryl-2-aminothiazole derivatives with an ethanone bridge at the N4 position of the piperazine residue found in fluoroquinolones. Purity and identity of the synthesized compounds were

confirmed by IR, ^{1}H-NMR, ^{13}C-NMR, and high-resolution mass spectral data besides elemental analysis.

2 | Methods

2.1 | Chemistry

Ciprofloxacin hydrochloride (CAS number: 85721–33-1) was donated by Atabay. Norfloxacin (CAS number: 70458–96-7), all starting materials, reagents, and solvents were of high-grade commercial products purchased from Sigma Aldrich or Merck. Compounds **13**, **14**, and acetazolamide were commercially supplied from Sigma Aldrich. While TLC studies of compounds **21–30** were carried out using chloroform: acetone (90:10, h/h), studies of compounds **31–40** were carried out using dichloromethane: ethyl acetate: ethanol (60:30:10 h/h/h) mobile phase. Melting points (°C, uncorrected) were determined using Schmelzpunktbestimmer SMP II basic model melting point apparatus. Elemental analysis was performed using the LECO CHNS-932 instrument, and the results were found to be consistent with the assigned structures. Infrared spectra were recorded on a Shimadzu FTIR 8400S, and data are expressed in wavenumbers, ν (cm^{-1}). ^{1}H- and ^{13}C NMR (decoupled) spectra were recorded on Bruker AVANCE-DPX 400 at 300 MHz; the chemical shifts were expressed in δ (ppm) downfield from tetramethylsilane (TMS) using DMSO-d_6 as solvent. High-resolution mass spectra were acquired using Jeol JMS700 instrument.

2.2 | General Procedure for the Synthesis of Compounds 1–5

0.001 mol of 2-bromo-4′-substituted acetophenone compound and 0.002 mol of thiourea are mixed in 15 mL of isopropanol at room temperature on a magnetic stirrer for 2 h. The reaction medium is neutralized by treatment with $NaHCO_3$ solution (5%, w/v). The crude product is first washed with a large amount of water, and after drying, it is purified by crystallization with a suitable solvent. Analytical data of compounds **1–5** are given in the Data S1.

2.3 | General Procedure for the Synthesis of Compounds 11, 12, and 15

2.3.1 | Method for Compounds 11 and 12

Concentrated HCl (20 mL), 0.026 mol of carboxylic acid (formic acid or acetic acid) and 0.022 mol of thiosemicarbazide were heated under reflux for 5 h. The reaction is monitored by TLC. After the reaction is complete, the medium was neutralized with a 40% NaOH solution. After the precipitated product is filtered, it is washed or crystallized with ethanol.

2.3.2 | Method for Compound 15

Acetazolamide (0.02 mol) was dissolved in 4 mL of HCl and 60 mL of anhydrous ethanol and heated under reflux at 80°C for approximately 4 h. After ethanol was partially evaporated, the resulting suspension was allowed to cool. The precipitated product was recrystallized from water.

Analytical data of compounds **11, 12**, and **15** are given in the Data S1.

2.4 | General Procedure for the Synthesis of Compounds 6–10 and 16–20

0.001 mol of amine compound (compounds **1–5** and **11–15**) is dissolved in dichloromethane (DCM) or dimethylformamide (DMF) in the presence of 0.002 mol of triethylamine (TEA). 0.0015 mol α-chloroacetylchloride is added very slowly to the reaction medium and stirred at room temperature for 2 h. The reaction is followed by TLC, and the product is obtained by evaporating the solvent. The crude product is purified by crystallization with a suitable solvent. Analytical data of compounds **6–10** and **16–20** are given in the Data S1.

2.5 | General Procedure for the Synthesis of Compounds 21–30 and 31–40

0.001 mol of the acetamide derivative (**6–10** and **16–20**) and 0.001 mol of norfloxacin or ciprofloxacin are mixed by dissolving separately in *N*,*N*-DMF. 0.0015 mol $NaHCO_3$ is added to the medium. The reaction mixture is stirred with heating not to exceed 70°C under reflux for 24 h. The reaction is followed by TLC. After the reaction is complete, the medium is neutralized with glacial acetic acid. After the precipitated product is filtered, it is washed with ethanol. Analytical data of compounds **21–40**, except compounds **31** and **35**, are given in the Data S1.

2.5.1 | 7-[4-(2-{[1,3,4-Thiadiazol-2-Yl]Amino}-2-Oxoethyl)piperazin-1-Yl]-1-Cyclopropyl-6-Fluoro-4-Oxo-1,4-Dihydroquinoline-3-Carboxylic Acid 31

Light brown powder. M.p. 166°C. Rf 0.29, Yield 28%. Elemental analysis calculated for $C_{21}H_{21}FN_6O_4S$. 2 H_2O; C 49.60, H 4.96, N 16.53, S 6.31; found C 49.53, H 4.91, N 17.13, S 6.67. IR (cm^{-1}): 3448, 3088 (O-H and N-H str); 1705, 1626 (C=O str). ^{1}H NMR (DMSO-d_6, 300 MHz) δ_H: 1.19–1.34 ppm (m, 4H, cyclopropyl-CH_2-); 2.73–2.89 ppm (m, 4H, piperazine H3, H5); 3.37–3.49 ppm (m, 6H, piperazine H2, H6 and -$COCH_2$ with water peak in DMSO-d_6); 3.83 ppm (s, 1H, cyclopropyl-CH); 7.57 ppm (d, 1H, *J* = *7.5 Hz*, Ar-H8); 7.94 ppm (d, 1H, *J* = *13.2 Hz*, Ar-H5); 8.65 ppm (s,1H, Ar-H2); 9.19 ppm (s,1H, thiadiazole -CH-); 12.41 ppm (s, 1H, amide NH); 15.21 ppm (s, 1H, -COOH). HRMS (ESI$^+$) *m/z* calculated/found: 472.1324/472.1328 (M$^+$).

2.5.2 | 7-[4-(2-{[5-Sulfamoyl-1,3,4-Thiadiazol-2-Yl] Amino}-2-Oxoethyl)piperazin-1-Yl]-1-Cyclopropyl-6-Fluoro-4-Oxo-1,4-Dihydroquinoline-3-Carboxylic Acid 35

Light yellow powder. M.p. > 350°C. Rf 0.47, Yield 72%. Elemental analysis calculated for $C_{21}H_{22}FN_7O_6S_2$. 5/2 H_2O; C 42.28, H 4.56, N 16.43, S 10.75; found C 41.86, H 4.57, N 16.55, S 10.65. IR (cm^{-1}): 3364, 3272, 3045 (O-H and N-H str); 1711, 1616 (C=O str). ^{1}H

TABLE 1 | Antituberculosis activity of fluoroquinolone derivatives **21–40** synthesized from ciprofloxacin and norfloxacin.

Compound	Lab ID codes	R_1	R_2	*M. tuberculosis* MIC (μg/mL)	Cytotoxicity (% inhibition[a])	Supercoiling assay (IC_{50}, in μM)
21	KUC140103	Adamantyl	Cyclopropyl	25	ND	ND
22	KUC140107	4-methoxyphenyl	Cyclopropyl	12.5	ND	ND
23	KUC140113	4-chlorophenyl	Cyclopropyl	**6.25**	**42.16**	ND
24	KUC140117	4-bromophenyl	Cyclopropyl	> 25	ND	ND
25	KUC140121	4-fluorophenyl	Cyclopropyl	25	ND	ND
26	KUC140104	Adamantyl	Ethyl	12.5	ND	ND
27	KUC140108	4-methoxyphenyl	Ethyl	> 25	ND	ND
28	KUC140114	4-chlorophenyl	Ethyl	> 25	ND	ND
29	KUC140118	4-bromophenyl	Ethyl	> 25	ND	ND
30	KUC140122	4-fluorophenyl	Ethyl	> 25	ND	ND
31	KUC140132	-H	Cyclopropyl	**6.25**	**21.56**	ND
32	KUC140129	$-CH_3$	Cyclopropyl	> 25	ND	ND
33	KUC140135	$-C_2H_5$	Cyclopropyl	12.5	ND	ND
34	KUC140140	$-CF_3$	Cyclopropyl	**6.25**	**18.78**	ND
35	KUC140137	$-SO_2NH_2$	Cyclopropyl	**1.56**	**9.54**	**5.6 ± 0.16**
36	KUC140133	-H	Ethyl	12.5	ND	ND
37	KUC140130	$-CH_3$	Ethyl	12.5	ND	ND
38	KUC140136	$-C_2H_5$	Ethyl	> 25	ND	ND
39	KUC140141	$-CF_3$	Ethyl	> 25	ND	ND
40	KUC140138	$-SO_2NH_2$	Ethyl	12.5	ND	ND
Ciprofloxacin				1.56	31.54	11.2 ± 0.98
Norfloxacin				3.125	22.64	13.56 ± 1.64

Note: Values written in bold indicate the most active compounds.
[a]At 25 μg/mL on RAW 264.7 cell line.

NMR (DMSO-d_6, 300 MHz) δ_H: 1.20–1.36 ppm (m, 4H, cyclopropyl CH_2); 2.73 ppm (bs, 4H, piperazine H3, H5); 3.36–3.55 ppm (m, 6H, piperazine H2, H6 and $-COCH_2$ with water peak in DMSO-d_6); 3.84 ppm (s, 1H, cyclopropyl CH); 7.53–7.98 ppm (m, 2H, Ar-H8, H5); 8.34 ppm (bs, 2H, $-SO_2NH_2$); 8.66 ppm (s,1H, Ar-H2); 15.22 ppm (s, 1H, -COOH). HRMS (ESI^+) *m/z* calculated/found: 473.1402/473.1408 $[M + H\text{-}SO_2NH_2]^+$.

2.6 | Antimycobacterial Activity

MIC values of all newly synthesized fluoroquinolone derivatives against *M. tuberculosis* H37Rv were determined using the MABA method. Their cytotoxicity was assessed in eukaryotic RAW 264.7 mouse macrophages, while the DNA supercoiling activity of these compounds was evaluated using Mtb-specific assay kits (Inspiralis Ltd., Norwich, UK). Results are offered in Table 1. Compound **35**, demonstrating the strongest antitubercular potential, was tested under nutrient starvation conditions in *M. tuberculosis* H37Rv cultures grown in Middlebrook 7H9 medium supplemented with OADC (Figure 2). Detailed experimental procedures are provided in the Data S1.

2.7 | Antibacterial and Antifungal Activity

The antibacterial and antifungal activities of compounds **21–40**, along with standard reference drugs, were initially assessed using the agar well diffusion method against a panel of microbial strains: *Escherichia coli* (*E. coli*) ATCC35218, *Yersinia pseudotuberculosis* (*Y. pseudotuberculosis*) ATCC911, *Klebsiella pneumoniae* (*K. pneumoniae*) ATCC13883, *Pseudomonas aeruginosa* (*P. aeruginosa*) ATCC43288, *Staphylococcus aureus* (*S. aureus*) ATCC25923, Methicillin-resistant clinical strain *of Staphylococcus aureus* (MRSA), *Enterococcus faecalis* (*E. faecalis*) ATCC29212, *Listeria monocytogenes* (*L. monocytogenes*) ATCC 43251, *Bacillus cereus* (*B. cereus*) 709 Roma, *Mycobacterium smegmatis* (*M. smegmatis*) ATCC607, *Candida albicans* (*C. albicans*) ATCC60193, and *Saccharomyces cerevisiae* (*S. cerevisiae*) RSKK 251 (See

Compound tested	Log reduction	MIC (μg/mL)
Compound **35** (KUC140137)	1.0 folds	1.56
Isoniazid	1.5 folds	-
Ciprofloxacin	1.8 folds	-
Rifampicin	1.8 folds	-
Moxifloxacin	2.0 folds	-

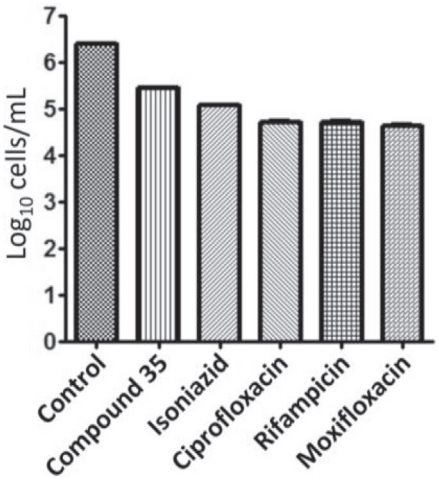

FIGURE 2 | Antimycobacterial activity of the compound **35** against *M. tuberculosis* in the nutrient starvation model. The bacterial count estimation (Mean ± SD, $n = 3$) for both control and treated groups was performed using the MPN assay. Compound **35** demonstrated a notable inhibition of *M. tuberculosis* growth in this model compared to the control ($p < 0.0001$), as analyzed through two-way ANOVA using GraphPad Prism Software.

Table S1, in the Data S1). The antimicrobial activities of all new fluoroquinolone derivatives were quantitatively evaluated in the respective broth media using the double microdilution method, and the MIC values (μg/mL) were determined in 96-well ELISA microplates (Barry et al. 1999). Results are offered in Table 2. Complete experimental details are provided in the Data S1.

2.8 | In Silico Studies

The molecular modeling studies of compound **35** were conducted against the crystal structures of DNA gyrase or type IIA topoisomerase from *M. tuberculosis* (PDB ID: 5BS8) and *S. aureus* (PDB ID: 2XCT) using the Schrödinger GLIDE module to better understand its interaction with type II topoisomerase (Ayipo et al. 2023b). To evaluate the stability of compound **35** within the protein structure under a solvent environment, a molecular dynamics (MD) simulation was carried out using the Desmond module of the Schrödinger LLC package (Abdelgawad et al. 2022; Farhan et al. 2022; Osmaniye et al. 2022; Shaw 2021). Detailed protocols of the *in silico* studies are provided in the Data S1.

3 | Results

3.1 | Design Strategy

Given the urgent need for novel antibacterial and antimycobacterial agents, hybrid molecules combining known bioactive motifs have gained increasing interest. The design strategy of the compounds **21–40** is given in Figure 1. In this study, thiazole and thiadiazole moieties, which are well documented for their broad antimicrobial and antimycobacterial activities (Foroumadi et al. 2006; Machado et al. 2018; Martínez-hoyos et al. 2016; Nandurkar et al. 2023; Shirude et al. 2013; Tatar et al. 2016), were selected for conjugation with two second-generation fluoroquinolones, ciprofloxacin and norfloxacin. The piperazine ring, particularly the N4 position, was chosen as the modification site due to its accessibility and tolerance for side-chain derivatization without significant loss of antimicrobial potency (Demirci et al. 2018).

To facilitate the conjugation, a 2-oxoethyl (acetyl) linker was introduced between the fluoroquinolone core and the heterocyclic moieties, ensuring optimal flexibility and spatial orientation for potential binding interactions with bacterial target enzymes. The design aimed to enhance the intrinsic activity of fluoroquinolones, improve their selectivity, and potentially overcome resistance mechanisms associated with DNA gyrase and topoisomerase IV inhibition (Froelich-ammon and Osheroff 1995; Nieto et al. 2005; Wiles et al. 2010).

Additionally, structural variations were introduced by modifying the R1 substituents on the azole rings (e.g., adamantyl, aryl, and sulfamoyl groups) to explore their effects on antimicrobial potency. Particular emphasis was placed on the thiadiazole derivatives, given previous findings indicating superior activity profiles compared to thiazole analogs (Demirci et al. 2018; Jazayeri et al. 2009; Martínez-hoyos et al. 2016; Shirude et al. 2013). This rational hybridization strategy was expected to produce compounds with both potent antibacterial and antimycobacterial activities, as validated by biological evaluation.

3.2 | Chemistry

Target molecules **21–40** were synthesized according to the synthetic route shown in Scheme 1. The 2-aminothiazole derivatives **1–5** used in our study were obtained from the reaction of bromomethylketones with thiourea and were converted into the corresponding chloroacetamide derivatives **6–10** by reaction with 2-chloroacetyl chloride. 2-Amino-1,3,4-thiadiazoles, compounds **11** and **12**, were obtained by refluxing formic acid or acetic acid with thiosemicarbazide in acidic medium. 2-Amino-1,3,4-thiadiazole derivatives carrying ethyl and trifluoromethyl substitutions at position 5 (compounds **13** and **14**, respectively) were obtained from commercial sources. 5-Sulfamoyl-1,3,4-thiadiazole-2-amine, compound **15**, was

TABLE 2 | Screening for antimicrobial activity of the compounds (MIC values in μg/μL).

		Microorganisms and minimal inhibitory concentration value (μg/mL)												
		Gram-negative bacteria				Gram-positive bacteria						No gram	Yeast-like fungi	
Compound	**Lab ID codes**	***E. coli***	***Y. pseu***	***K. pneu***	***P. aeu***	***S. aur***	***MRSA***	***E. fec***	***L. mon***	***L. acid***	***B. cer***	***M. smeg.***	***C. alb***	***S. cer***
21	KUC140103	5.22	20.90	41.80	83.59	83.59	167.19	167.19	167.19	—	167.19	20.90	—	—
22	KUC140107	2.59	20.70	10.35	82.81	10.35	10.35	41.41	10.35	—	10.35	10.35	—	—
23	KUC140113	1.29	20.70	10.35	82.81	10.35	10.35	20.70	20.70	—	10.35	5.18	—	662.50
24	KUC140117	2.49	19.92	19.92	79.69	19.92	19.92	39.84	39.84	—	39.84	19.92	—	318
25	KUC140121	681.25	10.64	5.32	85.16	21.29	10.64	21.29	21.29	—	5.32	5.32	—	—
26	KUC140104	19.92	19.92	39.84	159.38	79.69	79.69	159.38	318.75	318.75	318.75	39.84	318.75	—
27	KUC140108	39.45	78.91	78.91	252.5	315.63	315.63	252.5	252.5	—	252.5	—	—	—
28	KUC140114	39.45	157.81	157.81	631.25	315.63	315.63	—	—	—	631.25	—	—	631.25
29	KUC140118	20.12	80.47	40.23	321.88	80.47	80.47	321.88	321.88	—	160.94	—	—	321.88
30	KUC140122	21.09	168.75	84.38	—	168.75	168.75	337.50	—	—	168.75	—	—	337.50
31	KUC140132	<0.63	<0.63	<0.63	<0.63	5.08	2.54	20.31	20.31	20.31	5.08	162	—	650
32	KUC140129	5.03	20.12	40.23	80.47	10.06	20.12	80.47	80.47	—	40.23	10.06	—	—
33	KUC140135	<0.61	4.88	4.88	39.06	9.77	4.88	4.88	1.22	—	2.44	1.22	—	—
34	KUC140140	<0.64	1.28	1.28	20.51	1.28	5.13	10.25	20.51	—	2.56	1.28	—	328.13
35	KUC140137	<0.63	1.26	1.26	10.06	2.51	2.51	5.03	10.06	161.94	2.51	1.26	—	—
36	KUC140133	4.93	78.91	78.91	78.91	19.73	9.861	78.91	78.91	—	78.91	19.73	—	—
37	KUC140130	1.29	20.7	20.7	41.41	5.18	5.18	5.18	5.18	332.25	5.18	2.59	—	—
38	KUC140136	2.44	19.53	19.53	78.13	9.77	9.77	78.13	78.13	—	78.13	9.77	312.50	—
39	KUC140141	4.88	19.53	19.53	78.13	9.77	4.88	19.53	19.53	—	9.77	4.88	—	312.50
40	KUC140138	5.22	41.80	20.90	83.59	41.80	41.80	83.59	41.80	—	41.80	10.45	334.38	—
Norfloxacin		<0.6	0.6	1.32	5.27	1.32	0.6	2.64	2.64	675	2.64	5.27	—	—
Ciprofloxacin		<0.6	0.6	0.6	1.31	1.31	1.31	2.61	1.31	83.59	1.31	<0.6	—	—

Note: Y. pseu: *Y. pseudotuberculosis* ATCC 911, K. pneu; *K. pneumoniae* ATCC13883, P. aeu: *P. aeruginosa* ATCC 43288, S. aur: *S. aureus* ATCC 25923, MRSA; Methicillin-resistant *S. aureus*, E. fae: *E. faecalis* ATCC 29212, L. mon; *L. monocytogenes* ATCC43251, L. aci; *L. acidophilus* RSKK 06029, B. cer: *B. cereus* Roma 709, M. smeg: *M. smegmatis* ATCC607, C. alb: *C. albicans* ATCC 60193, S. cer; *S. cerevisiae* RSKK 251, (—): no activity.

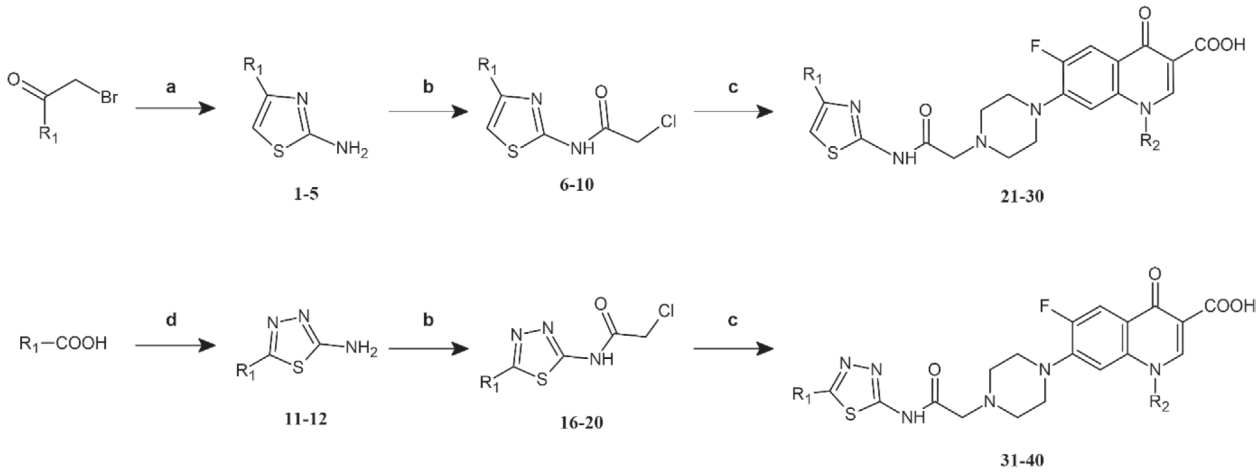

Compound	R_1	Compound	R_1	R_2	Compound	R_1	R_2
1, 6	adamantyl	**21**	adamantyl	cyclopropyl	**26**	adamantyl	ethyl
2, 7	4-methoxyphenyl	**22**	4-methoxyphenyl	cyclopropyl	**27**	4-methoxyphenyl	ethyl
3, 8	4-chlorophenyl	**23**	4-chlorophenyl	cyclopropyl	**28**	4-chlorophenyl	ethyl
4, 9	4-bromophenyl	**24**	4-bromophenyl	cyclopropyl	**29**	4-bromophenyl	ethyl
5, 10	4-fluorophenyl	**25**	4-fluorophenyl	cyclopropyl	**30**	4-fluorophenyl	ethyl
11, 16	H	**31**	H	cyclopropyl	**36**	H	ethyl
12, 17	methyl	**32**	methyl	cyclopropyl	**37**	methyl	ethyl
13, 18	ethyl	**33**	ethyl	cyclopropyl	**38**	ethyl	ethyl
14, 19	trifluoromethyl	**34**	trifluoromethyl	cyclopropyl	**39**	trifluoromethyl	ethyl
15, 20	sulfamoyl	**35**	sulfamoyl	cyclopropyl	**40**	sulfamoyl	ethyl

SCHEME 1 | Synthetic route to target fluoroquinolones **21–40**. Key to reagents and conditions: (a) thiourea, isopropanol, rt.; (b) $ClCH_2COCl$, TEA, DCM; (c) CFX/NFX, $NaHCO_3$, DMF; (d) thiosemicarbazide, conc. HCl, reflux. Compounds **13** and **14** were commercially supplied; compound **15** were prepared as described in experimental section.

obtained from the hydrolysis of commercially available acetazolamide in acidic medium. In the next step, compounds **11–15** were reacted with 2-chloroacetyl chloride to obtain chloroacetamides **16–20**.

The obtained chloroacetamides **6–10** and **16–20** were reacted with norfloxacin and ciprofloxacin in DMF in a weakly basic medium in the last step, and target molecules **21–40** were synthesized. Following the isolation process, the crude products were crystallized from appropriate solvents. The purity of the synthesized compounds was checked by TLC and elemental analysis, and their structures were confirmed by IR, ^{1}H NMR, ^{13}C NMR, and mass spectral data.

The vibrational frequencies identified by FTIR analysis of the target compounds **21–40**, notably the carboxylic acid C=O stretching (1738–1700 cm^{-1}), the conjugated ketone C=O stretching (1705–1684 cm^{-1}), the amide C=O stretching (1630–1616 cm^{-1}), and the broad O-H/N-H stretching bands (3448–3032 cm^{-1}), exhibit strong concordance with the spectral data previously reported for structurally analogous fluoroquinolone and azole derivatives (Abdel-aziz et al. 2013; Foroumadi et al. 2003; Kulabaş et al. 2022; Mohammed et al. 2016; Pandit et al. 2016). This correlation with established literature values reinforces the reliability of the functional group assignments and substantiates the structural elucidation of the target compounds. The remaining vibration bands were observed at expected regions.

^{1}H-NMR spectra of compounds **21–40** showed proton signals corresponding to carboxylic acid groups as singlets at 15.65–15.14 ppm, while acetamide NH protons appeared as singlets at 12.46–11.95 ppm. However, the NH peak corresponding to the acetamide group was not observed in the ^{1}H-NMR spectra of compounds **33**, **34**, **35**, **39**, and **40**, and it was thought that the relevant proton was replaced by D_2O. Singlets in the range of 8.96–8.65 ppm were attributed to the H2 protons of the quinolone rings. Additionally, the H5 protons of the quinolone rings were observed as doublets at 7.97–7.82 ppm. Distinct doublets for the H8 protons of the quinolone rings were identified at 7.65–7.19 ppm. The quinolone H5 and H8 protons were found to couple with fluorine atoms at the 6th position of the ring, with coupling constants for the H5 protons calculated as J = 13.2 Hz and for the H8 protons as J = 7.82–7.97 Hz. The piperazine H_2, H_6, and -$COCH_2$ peaks were observed at 3.33–3.61 ppm with the water peak in DMSO-d_6. Finally, SO_2NH_2 protons were detected at 8.34 ppm for compounds **35** and **40**. The ^{1}H NMR results for compounds **21–40** were consistent with literature reports (Abdel-aziz et al. 2013; Foroumadi et al. 2003; Kulabaş et al. 2022; Mohammed et al. 2016; Pandit et al. 2016).

When the ^{13}C-NMR spectra of compounds **23**, **28**, **32**, and **37** were examined, the signals corresponding to the conjugated ketone carbons of the quinolone rings were observed at 176.07–176.27 ppm. Moreover, the carboxylic acid groups were identified by peaks at 165.87–166.24 ppm (Türe et al. 2019). These spectra confirmed our target structure by a previously absent carbonyl (C=O) peak of the acetamide group within the range of 168.42–168.81 ppm. While C-2 carbons of the quinolone ring resonated between 145.16–145.50 ppm, C-6 carbons were detected in the range of 152.86–153.51 as doublets with robust coupling constants of 247.5–255 Hz. Finally, -CH_2- carbon of

the acetamide moiety appeared at 59.69–59.79 ppm (Demirci et al. 2018). These findings are found to be consistent with the literature.

To confirm the structure of synthesized compounds, HMBC spectra of selected compounds **23**, **28**, **32**, and **37** were examined. The interactions of the carbonyl group of acetamide with the H3 and H5 protons (2.73–2.80 ppm) on the piperazine ring confirmed that this carbon resonated in the range 168.42–168.81 ppm. Also, the peak observed in the range 165.87–166.24 ppm was attributed to the carbonyl of carboxylic acid, due to its contour with the H2 proton of the quinolone ring around 8.66 and 8.96 ppm. The peak observed around 176.07–176.27 ppm was attributed to the carbonyl of the ketone group, due to its contour with the H2 and H8 (7.19–7.58 ppm) protons (See Data S1).

High-resolution ESI mass spectra of compounds **21–40** were recorded and confirmed their molecular weights. The mass analysis of the synthesized compounds gave $[M+Na]^+$ and $[M+K]^+$ ion peaks, besides correct molecular ion peaks corresponding to $[M+H]^+$. Among the synthesized compounds, for compounds **35** and **40**, which contain a sulfamoyl residue, instead of the molecular ion peak, the $[M+H\text{-}SO_2NH_2]^+$ peak was detected.

Of the synthesized fluoroquinolone–thiadiazole hybrids, compound **32** was synthesized using the same method as described by Pandit et al. (2016). Due to a difference in the melting point of this compound compared to the reported value, we provided a complete structural characterization, including ^{13}C-NMR and elemental analysis, which were not included in the mentioned study. Additionally, we evaluated the antibacterial activity of compound **32** against a broader spectrum of bacteria. Moreover, this study presents for the first time the antibacterial and antituberculosis activities, DNA gyrase inhibition, and molecular modeling studies of both the previously reported and newly synthesized fluoroquinolone derivatives.

3.3 | Biological Studies

3.3.1 | Antimycobacterial Activity Studies

All synthesized compounds **21–40** were screened for their antimycobacterial activity against *M. tuberculosis H37Rv* strain using microplate alamar blue assay (MABA) and their MIC results were determined (Table 1). Ciprofloxacin and norfloxacin were used as reference drugs for comparison of the antituberculosis activity results of the compounds **21–40**. Twelve fluoroquinolone derivatives out of twenty synthesized target compounds exhibited antimycobacterial activity by a MIC value of 25 μg/mL or lower. The MIC values of the active compounds ranged from 1.56 to 25 μg/mL. The remaining eight compounds with MICs higher than 25 μg/mL were assumed to be inactive and were excluded from further studies.

Cytotoxicity studies were conducted only for four target molecules (compounds **23**, **31**, **34**, and **35**) with MIC values of 6.25 μg/mL or less. For this purpose, the % inhibition values of the compounds applied at a concentration of 25 μg/mLon the RAW 264.7 cell line were determined, and it was observed that compounds **31**, **34**, and **35** induced 21.56, 18.78, and 9.54% inhibition, respectively. These cytotoxicity rates were lower than those of ciprofloxacin and norfloxacin, indicating that compounds **31**, **34**, and **35** are more reliable in terms of selective toxicity against the mycobacterial pathogen. According to the screening results, compounds **23**, **31**, **34**, and **35** were identified as the most active representatives of the target compounds.

When the structure–activity results obtained against *M. tuberculosis* H37Rv were evaluated, it was clearly seen that ciprofloxacin derivatives exhibited lower MIC values on average compared to the norfloxacin derivatives. On the other hand, thiadiazole ring attachment in both ciprofloxacin and norfloxacin derivatives resulted in higher activity than thiazole hybrids. It is noteworthy that the most active derivatives emerged in compounds **31–35**, in which the thiazole ring was conjugated with ciprofloxacin.

Compound **35**, which had the strongest antitubercular effect, was found to have the same potency as ciprofloxacin (MIC = 1.56 μg/mL) and was twice as effective as norfloxacin. However, this compound exhibited a cytotoxicity profile that was three times safer than ciprofloxacin and two times safer than norfloxacin. Compound **35**, which emerges as the lead compound in this study, was selected for the DNA gyrase supercoiling assay. The supercoiling assay was also conducted for reference drugs norfloxacin and ciprofloxacin. As a result of this assay, the IC_{50} value of compound **35** was found to be 5.6 ± 0.16 μM, and it was found to be more effective against the DNA gyrase enzyme than the reference drugs.

In our previous study conducted by Kulabaş et al., the compound with the structure 7-{4-([{4-sulfamoylphenyl} amino]-2-oxoethyl)piperazin-1-yl}-1-cyclopropyl-6-fluoro-4-oxo-1,4-dihydroquinoline-3-carboxylic acid was determined to be the most effective molecule against *M. tuberculosis* H37Rv strain (Kulabaş et al. 2022). When we compare this molecule with compound **35** in our current study, its structural common points are that it is derived from ciprofloxacin, carries an N-aryl acetamide side chain in the 4th position of the piperazine ring, and carries a sulfamoyl residue. It is noteworthy that both compounds have the lowest MIC value in their series, a lower toxicity profile than the reference drugs, and high activity against the DNA gyrase enzyme. The contribution of the sulfamoyl group in binding to the target enzyme is discussed in the molecular docking section.

3.3.2 | Nutrient Starvation Model

Mycobacterium tuberculosis (Mtb) can exist in an asymptomatic state, showing its growth only when the host's immune system is weakened. New medications should target the effectiveness against this type of Mtb, commonly known as latent or dormant TB. Dormancy in bacteria is induced through a nutrient starvation model by subjecting the culture to PBS deprivation for a period of 6 weeks. The nutrient starvation model has been previously validated as a reliable method to mimic the non-replicating persistent state of *Mycobacterium tuberculosis*

and has been successfully utilized in earlier studies (Kulabaş et al. 2022; Wayne and Hayes 1996). Therefore, this model provides relevant insights into the potential efficacy of compound **35** against latent TB infections.

To evaluate the potential inhibitory activity of compound **35** (KUC140137) against dormant mycobacterial forms, the nutrient starvation model was employed at a concentration of 10 μg/mL (Figure 2). Compound **35** demonstrated inhibition with a log reduction of 1.0-fold, whereas isoniazid, ciprofloxacin, rifampicin, and moxifloxacin, all at equivalent concentrations, exhibited log reductions of 1.5, 1.8, 1.8, and 2.0, respectively, in comparison to the control. This implies that compound **35** had some impact on the dormant type of *M. tuberculosis* strain while showing promising activity against actively growing mycobacteria.

3.3.3 | Antimicrobial Activity Studies

The antibacterial activity of the synthesized fluoroquinolone hybrids of thiazoles **21–30** and thiadiazoles **31–40** on Gram-positive, Gram-negative, and non-Gram-stainable bacterial strains as well as yeast-like fungi was examined using agar-well diffusion (Table S1; see in the Data S1) and microdilution (Table 2) techniques. It was observed that among the test compounds, those forming larger zone diameters also had lower MIC values.

The majority of the synthesized compounds exhibited a spectrum of antimicrobial activity with varying proportions against the bacterial species tested. While all synthesized compounds **21–40** exhibited a higher activity profile, especially against Gram-negative pathogen groups, they were not effective against *L. acidophilus*, which represents a group of beneficial bacteria in the flora. Compound **31** derived from ciprofloxacin was identified as the most potent antimicrobial agent with a MIC of <0.63 μg/μL for all Gram-negative bacteria tested (Table 2). This value is comparable to ciprofloxacin and norfloxacin used as standard drugs. While compounds **34** and **35**, which are thiadiazole-CIP hybrids, showed MIC values of 1.28 and 2.51 μg/mL, respectively, against *S. aureus*, compound **35** was identified as the most effective derivative against the MRSA strain.

The fact that the synthesized fluoroquinolone derivatives were not effective against *Candida* species demonstrated the selective and mechanistic effects of these molecules. The marginal or no effect of these molecules against *Lactobacillus acidophilus* confirmed that they are germicidal only against pathogens. Since potent antibiotics have disruptive effects on the intestinal flora, the lack of antibacterial effect of compound **21–40** against non-pathogenic *L. acidophilus* makes them more advantageous than existing antibiotics. Additionally, it is noteworthy that derivatives that are effective against *Mycobacterium smegmatis* were also found to be effective against *M. tuberculosis*. It was determined that compounds **33**, **34**, and **35**, which were the most effective against *M. smegmatis*, were also effective against *M. tuberculosis*.

The most effective derivatives against both Gram-negative and Gram-positive bacteria were compounds **31–35**, which are thiadiazole-ciprofloxacin hybrids, as they presented lower MIC values against both Gram-positive and Gram-negative bacteria. This series also includes the most potent derivatives against *S. aureus* and MRSA strains. In particular, the MIC of compound **34** against *S. aureus* of 1.28 μg/mL is almost the same as that of ciprofloxacin and norfloxacin used as references.

The 20 synthesized molecules can be classified into four structural types: thiazole–CIP, thiazole–NOR, thiadiazole–CIP, and thiadiazole–NOR. When the activities of these groups are compared according to the antibacterial screening results, their average potencies can be ranked as: thiadiazole-CIP > thiadiazole-NOR > thiazole-CIP > thiazole-NOR for both Gram-negative and Gram-positive strains.

Compound **31** was identified as the most promising lead compound for antibacterial screening, with the lowest MIC values (<0.63 μg/mL), particularly against Gram-negative bacteria. This broad-spectrum compound was also among the most effective compounds against Gram-positive *S. aureus* and MRSA strains.

3.4 | Structure–Activity Relationship (SAR) Analysis

The antimicrobial and antimycobacterial activities of the synthesized fluoroquinolone-azole hybrids (compounds **21–40**) revealed several important structure–activity relationships:

- *Nature of the heterocyclic moiety*: Compounds bearing thiadiazole rings exhibited overall higher antimycobacterial and antibacterial activities than their thiazole analogs, suggesting the superior bioactivity of thiadiazole scaffolds in this series.
- *Core fluoroquinolone structure*: Ciprofloxacin-based derivatives were generally more potent than their norfloxacin counterparts, highlighting the beneficial effect of the cyclopropyl substitution at position 1 on the quinolone core.
- *Effect of R1 substituents*: Substituents on the azole moiety significantly influenced biological activity. In particular, the presence of a sulfamoyl group (as in compound **35**) markedly enhanced both antimycobacterial and antibacterial effects, likely due to improved binding affinity to the DNA gyrase enzyme.
- *Hydrophobic substituents*: Adamantyl and aryl substitutions (e.g., 4-chlorophenyl and 4-bromophenyl) generally conferred moderate activity, although no consistent trend favoring bulky hydrophobic groups was observed across all assays.
- *Activity spectrum*: Compounds with thiadiazole structures (especially **31–35**) displayed broad-spectrum antibacterial activity, effective against both Gram-positive and Gram-negative bacteria, while maintaining selectivity by sparing non-pathogenic *Lactobacillus* strains and yeast-like fungi.

Overall, the findings indicated that hybridization with thiadiazole units, maintaining a ciprofloxacin core, and introducing polar functional groups such as sulfamoyl were favorable strategies for enhancing antibacterial and antimycobacterial potency.

3.5 | In Silico Studies

3.5.1 | Molecular Docking

To gain a deeper understanding of the molecular interactions involved, docking studies were performed with both *M. tuberculosis* DNA gyrase (PDB ID: 5BS8) and *S. aureus* DNA gyrase (PDB ID: 2XCT). These studies aimed to explore the binding interactions of the compounds with the active sites of each enzyme, providing insights into specific residues and binding modes that contribute to the compounds' inhibitory potential. Fluoroquinolones interact with DNA gyrase with particular domains and conformations, preventing catalysis of DNA strand passage and stabilizing DNA-enzyme complexes that impede the DNA replication process and cause double breaks in the DNA, resulting in their bactericidal effect. The most active compound, **35**, was subjected to molecular docking simulations using Schrödinger Glide software based on its potential antimycobacterial actions. The binding interaction of the compound, **35,** is completely consistent with the mode of action of fluoroquinolones. Compound **35** binds in the middle of the two active sites, with the fluoroquinolone scaffold positioned between the stretched DNA's two central base pairs.

For the proteins 5BS8 and 2XCT, the Glide docking score of compound **35** was found to be −10.563 kcal/mol and −8.544 kcal/mol, respectively. Maestro's ligand interaction tool was used to generate the 2D and 3D graphical representations of the ligand–protein interactions shown in Figure 3. The 2D diagram showed a crucial hydrogen bond with Arg128 through the carboxylic group of the quinolone ring in the *M. tuberculosis* DNA gyrase target. Additionally, the amino group of terminal sulfonamide and the DNA nucleotide bases exhibit bidentate hydrogen bonding (DC *H*13 and DG *H*13). On the other hand, the quinolone scaffold forms Van der Waals contacts with the DA G11 and DA H15, notably π–π interactions, with binding energy of −12.578 kcal/mol and −10.958 kcal/mol, respectively, which is comparable to that of the reference moxifloxacin (Figure 3) (Blower et al. 2016).

The docking analysis of compound **35** in the active site of *S. aureus* DNA gyrase indicated that it was stabilized inside the active site through strong van der Waals contacts with the nucleotide bases of DNA DG G9 and DT E8 with binding energies of −8.461 kcal/mol and −12.542 kcal/mol, respectively. It also demonstrated an additional type of interaction with the nucleotide bases of DNA through bidentate hydrogen bonds (DA G11 and DA H11) (Figure 3). Compound **35** demonstrated similar binding interactions to co-crystallized ciprofloxacin, with the exception of a metal coordinate bond with the Mn^{+2} ion. Biochemical investigations suggested that the interaction with the Mn^{+2} ion greatly enhances rates of enzyme-mediated DNA breakage (Bax et al. 2010).

3.5.2 | MD Simulation

Because docking only provides a preparatory indication of a compound's fitness inside the active site of DNA gyrase from *M. tuberculosis* (5BS8) and *S. aureus* (2XCT), the binding poses of compound **35** were subjected to MD simulations, which enabled interpretation of the structural details, conformational flexibility, and stability of the protein–ligand complexes. The root mean square deviation (RMSD), root mean square fluctuation (RMSF), and radius of gyration (rGyr) of each of the MD trajectories were compared and assessed for stability. The RMSD is the mean deviation in atom displacement over time from the beginning (reference) frame in the protein–ligand complex. A lower RMSD value during the MD simulation indicates that the protein–ligand complex is more stable, while a higher RMSD value signifies that the protein–ligand complex is less stable (Ahmad et al. 2022a; Girase et al. 2022).

Figure 4 shows the RMSD of the Cα atoms of DNA gyrase protein throughout the simulation based on the reference frame backbone. The maximum RMSD value of protein Cα atoms of 5BS8-**35** complex is 3.59 Å, which indicates that the complex was maintained constantly during the simulation time. While 2XCT of the 2XCT-**35** complex exhibited minor conformational changes with an average RMSD value of 1.98 Å from 0 to 44 ns, it shifted to 2.5 Å around 45–64 ns and thereafter stabilized with a mean RMSD of 2.20 Å from 67 ns and over the simulation time. Both complexes exhibit a plateau in RMSD values and structural convergence during the first 12 ns of the 100 ns simulation period.

A further investigation of the structural flexibility of the protein–ligand complexes, as evaluated by RMSF, indicated that the 5BS8-**35** complex exhibited more noticeable variations, with residual indexes of 248–248, 485–488, 654–658, 730–733,

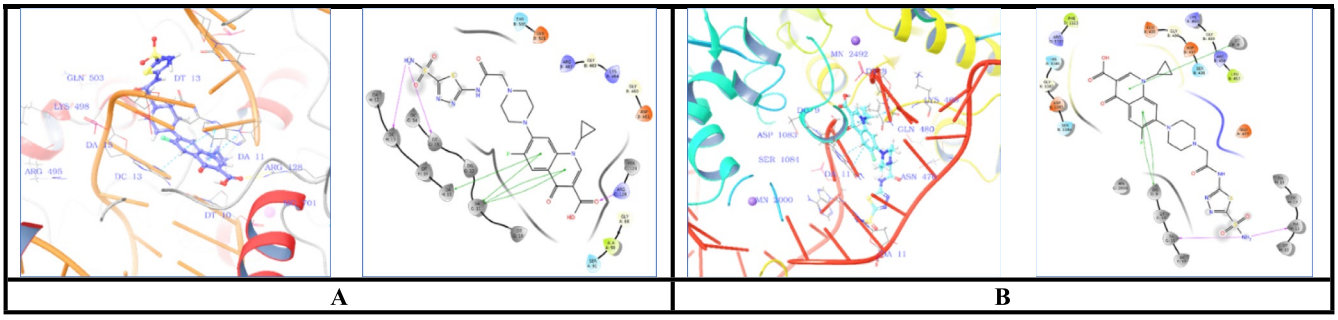

FIGURE 3 | (A) 3D and 2D diagrams illustrate the binding mode of compounds **35** interacted with the active site of *M. tuberculosis* DNA gyrase (PDB ID: 5BS8) enzyme. (B) 3D and 2D diagrams illustrate the binding mode of compounds **35** interacted with the active site of *S. aureus* DNA gyrase (PDB ID: 2XCT). *Hydrogen bonds are indicated by pink arrows, while π–π stacking interactions are shown as green lines.*

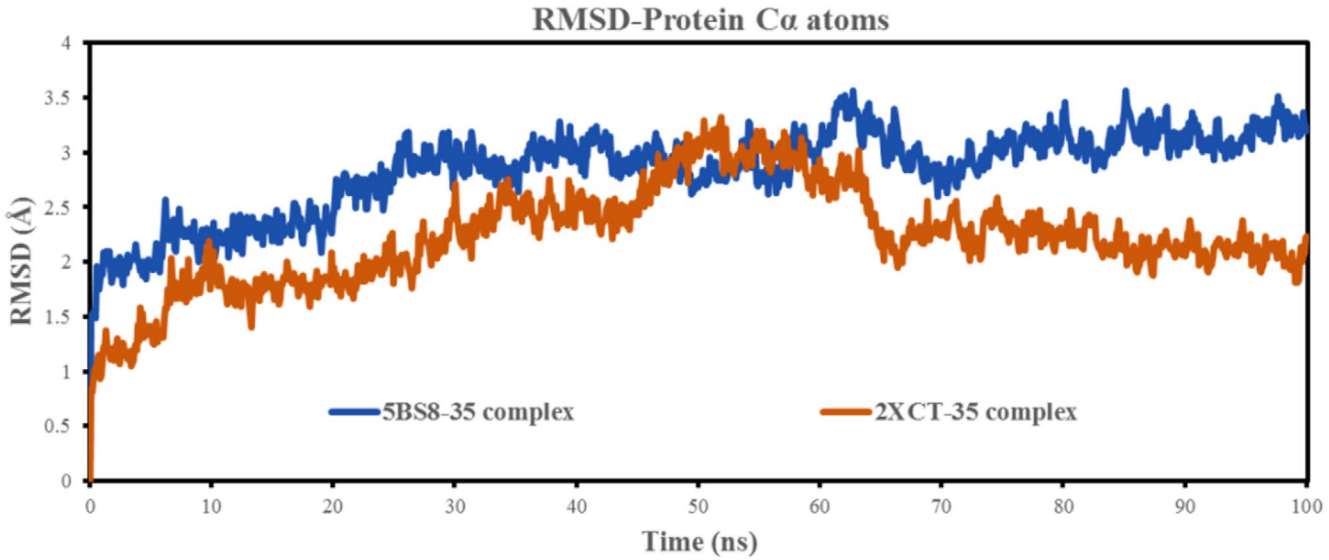

FIGURE 4 | Time-dependent RMSD plots of 5BS8-**35** complex (Blue) and 2XCT-**35** complex (orange) obtained from 100 ns MD simulation Trajectories.

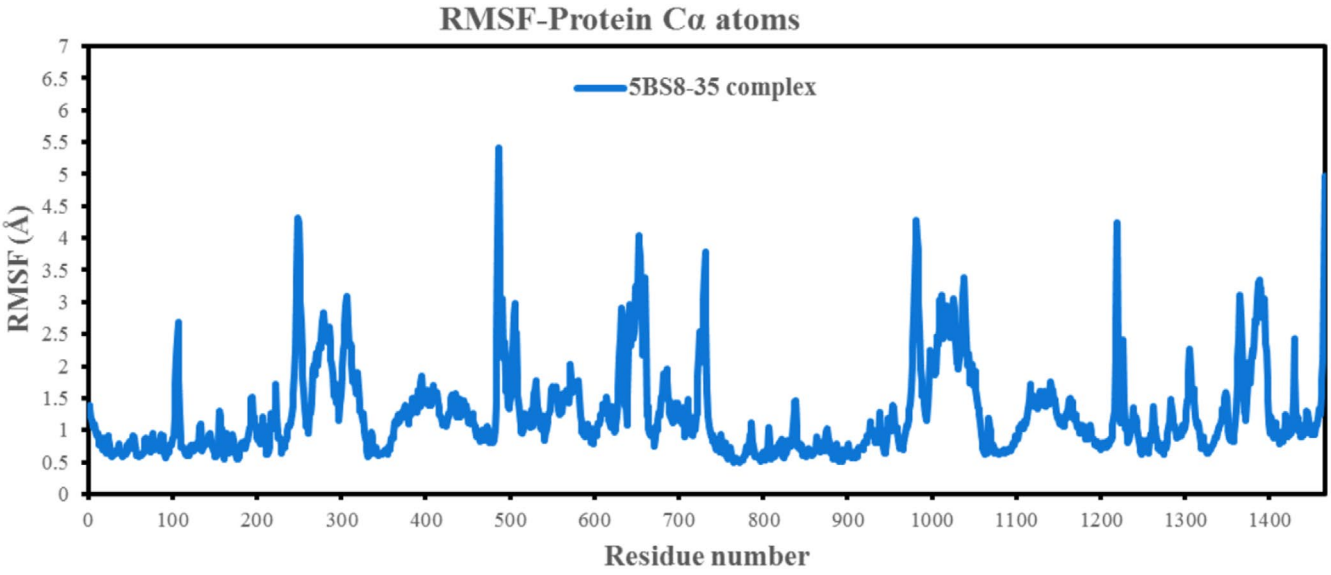

FIGURE 5 | RMSF of Cα atoms of the 5BS8-**35** complex where the ordinate is individual amino acid fluctuation (Å) and the abscissa is the residual number.

980–982, and 1219–1221, and RMSFs of 4.30 Å, 5.20 Å, 3.78 Å, 3.70 Å, 3.99 Å, and 4.24 Å, respectively. The remaining amino acid residues had lesser fluctuations with RMSF ranging between 0.6–3.5 Å (Figure 5). The amino acids that fluctuate more in the 2XCT-**35** complex during simulation include residual index 318–322, 576–569, 1092–1135, 1244–1247, and 1367–1375, all of which have RMSF greater than 3.5 Å. The amino acids that were stable and fluctuated less during simulation had an average RMSF of 0.40–3.0 Å (Figure 6). In general, large variations corresponding to RMSF values suggest greater flexibility and fewer stable bonds, while low fluctuations imply well-structured complex areas and fewer distinct bonds (more stable bonds) (Ghosh et al. 2021; Radwan et al. 2022). The minimal residue movement seen with the 5BS8 protein contributes to its structural stability, which is consistent with the RMSD finding in this study, where it was found to be the most stable in contrast to the 2XCT-**35** complex.

The radius of gyration (RGyr) of a protein–ligand complex system may be described as the distribution of atoms around its axis. One of the most crucial markers for forecasting a macromolecule's structural activity is the computation of RGyr, which represents oscillations in complex compactness (Ayipo et al. 2023a; Boulaamane et al. 2023; Zrieq et al. 2021). As a consequence, the stability of compound **35** in complex with the 5BS8 and 2XCT proteins was studied throughout a 100-ns simulation time, as shown in Figure 7. Smaller and more consistent changes in the compound **35** RGyr value revealed that the complex was stable and compact, resulting in increased interaction between 5BS8 and the ligand. The average RGyr for compound **35** in complex

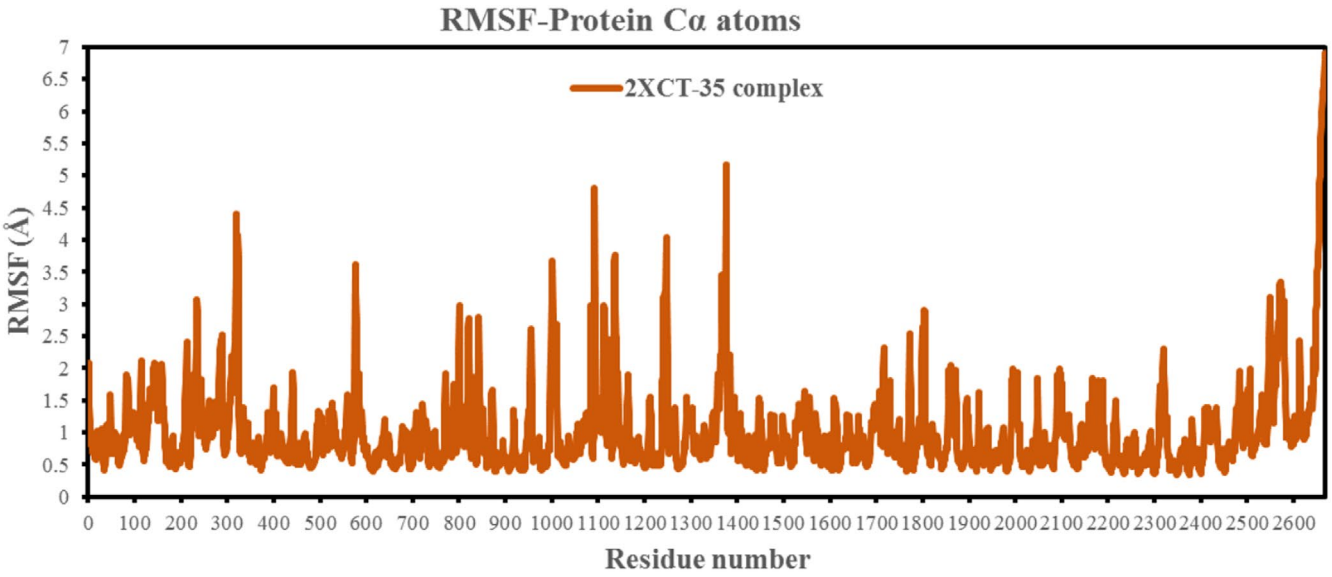

FIGURE 6 | RMSF of Cα atoms of the 2XCT-**35** complex where the ordinate is individual amino acid fluctuation (Å) and the abscissa is the residual number.

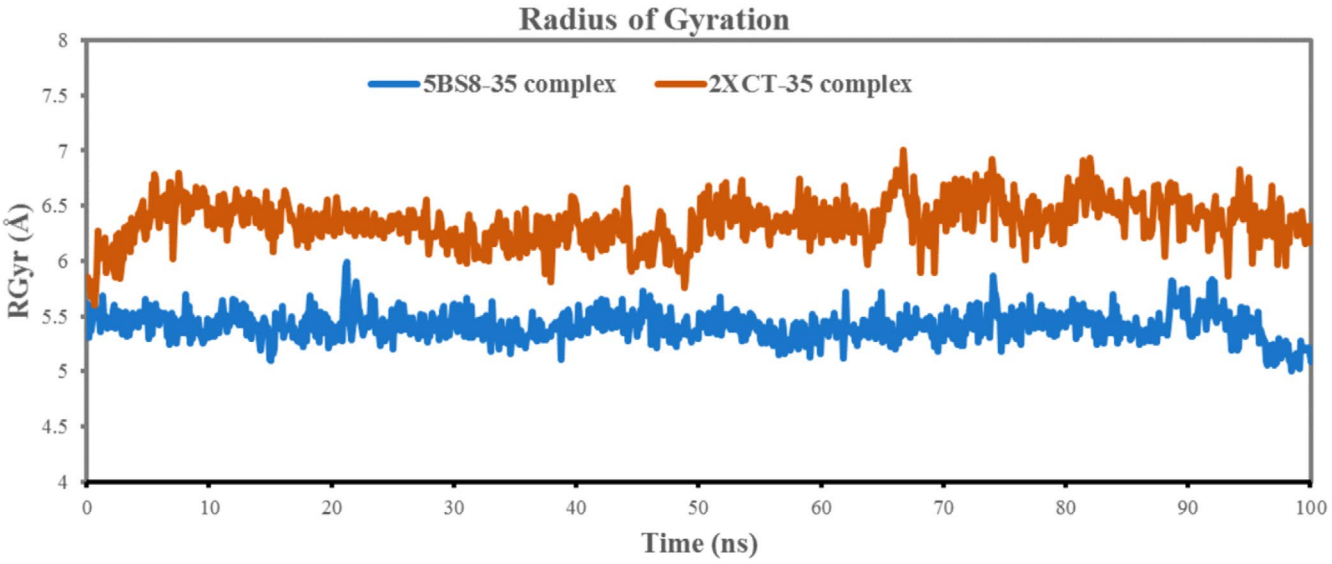

FIGURE 7 | Time-dependent radius of gyration (RGyr) plot of 5BS8-**35** complex (Blue) and 2XCT-**35** complex (orange), obtained from 100 ns MD simulation trajectories.

with 5BS8 and 2XCT was found to be 5.401 Å and 6.431 Å, respectively, indicating that the active site of the target proteins does not cause significant conformational changes.

To understand the protein motion in response to the ligand binding, principle component analysis (PCA) of Ca atoms was studied. PCA could project the high-dimensional protein dynamics into the low-dimensional space by extracting essential data points representing eigenvectors and eigenvalues that reflect the corresponding protein motion and the direction of motion (Ahmad et al. 2022b; Bharadwaj et al. 2022). The PCA score plot reveals different cluster formations (Figure 8). The 2XCT-**35** complex forms a broad cluster (orange), showing a substantial divergence in contrast to the 5BS8-**35** complex (blue). This is reasonable as compound **35** exhibits a minor divergence when a complex is formed with the 2XCT protein. In conclusion, the correlation between the PCA results and the RMSD and RMSF results strengthens the investigation's validity.

4 | Conclusion

Twenty new thiazole/thiadiazole-fluoroquinolone conjugates with potential antibacterial and antituberculous effects were designed and synthesized. According to structure–antibacterial effect relationships, ciprofloxacin derivatives were more effective than norfloxacin derivatives. On the other hand, thiadiazole derivatives were also found to be more effective than thiazole derivatives. The target compounds appeared overall more effective against Gram-negative bacteria than Gram-positive bacteria. The most effective derivative in the antibacterial effect screening was compound **31**, which is a thiadiazole-ciprofloxacin

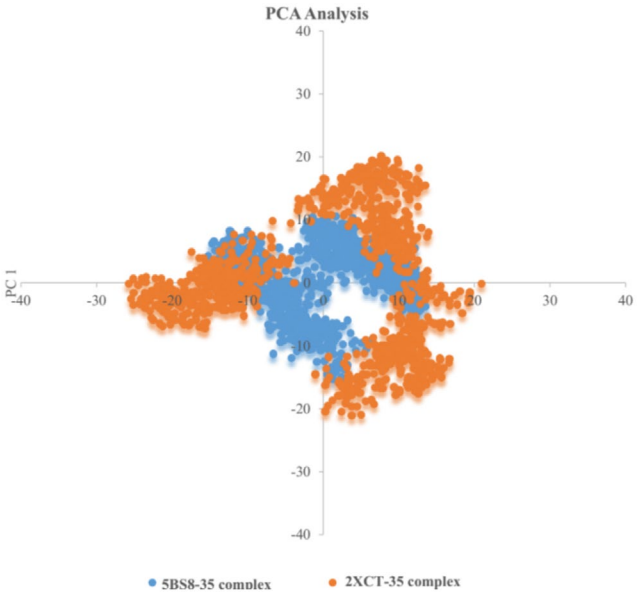

FIGURE 8 | Two-dimensional projection of the motion of the trajectory of 5BS8-**35** complex and 2XCT-**35** complex over the PC1 and PC2.

hybrid and does not contain substituents at the R_1 position. The fact that the molecules found to have potent antibacterial effects did not show any effect against yeast-like fungi and the non-pathogenic *L. acidophilus* strain was an indication that the effect of these compounds was selective.

While norfloxacin derivatives were found to be low or ineffective in antimycobacterial effect studies conducted on *M. tuberculosis* H37Rv strain, the most effective derivatives were from the thiadiazole-ciprofloxacin series. Of these, the most promising molecule was compound **35**, which is a thiadiazole-ciprofloxacin hybrid and contains a sulfamoyl residue at the R_1 position. Further studies on compound **35** demonstrated that this lead compound inhibits DNA gyrase with a lower IC_{50} than ciprofloxacin and norfloxacin and exhibits lower toxicity towards RAW 264.7 macrophages. Studies using the nutrient starvation model revealed that compound **35** also exerted a remarkable effect against dormant-type *M. tuberculosis*, although not as much as the reference drugs.

In silico molecular docking studies with *S. aureus* DNA gyrase (PDB ID: 2XCT) and *M. tuberculosis* DNA gyrase (PDB ID: 5BS8) show that compound **35** binds to the middle of the two active sites, with the fluoroquinolone residue located between the two central DNA base pairs. For the validity of docking studies, a 100-ns MD simulation was performed. According to the PCA analysis results, the stability of the complexes formed between compound **35** and the DNA gyrase proteins of *M. tuberculosis* and *S. aureus* was demonstrated.

Acknowledgments

This research was supported by Marmara University Scientific Research Projects Commission with grant number SAG-C-DRP-140115-0002. The authors are grateful to Dr. Jürgen Gross from the Institute of Organic Chemistry, University of Heidelberg, for his generous help in obtaining high-resolution mass spectra of the compounds. Ciprofloxacin hydrochloride was generously donated by Atabay Pharmaceuticals and Fine Chemicals Inc.

Conflicts of Interest

The authors declare no conflicts of interest.

Data Availability Statement

The data that supports the findings of this study are available in the Data S1 of this article.

References

Abdel-aziz, M., S. Park, G. E. A. A. Abuo-rahma, M. A. Sayed, and Y. Kwon. 2013. "Novel N -4-Piperazinyl-Ciprofloxacin-Chalcone Hybrids: Synthesis, Physicochemical Properties, Anticancer and Topoisomerase I and II Inhibitory Activity." *European Journal of Medicinal Chemistry* 69: 427–438. https://doi.org/10.1016/j.ejmech.2013.08.040.

Abdelgawad, M. A., J. M. Oh, D. G. T. Parambi, et al. 2022. "Development of Bromo- and Fluoro-Based α, β-Unsaturated Ketones as Highly Potent MAO-B Inhibitors for the Treatment of Parkinson's Disease." *Journal of Molecular Structure* 1266: 133545. https://doi.org/10.1016/j.molstruc.2022.133545.

Ahmad, I., R. H. Pawara, R. T. Girase, et al. 2022a. "Synthesis, Molecular Modeling Study, and Quantum-Chemical-Based Investigations of Isoindoline-1, 3-Diones as Antimycobacterial Agents." *ACS Omega* 7: 21820–21844. https://doi.org/10.1021/acsomega.2c01981.

Ahmad, I., S. Rahman, M. Shaikh, R. Pawara, S. N. Manjula, and H. Patel. 2022b. "Synthesis, Molecular Modelling Study of the Methaqualone Analogues as Anti-Convulsant Agent With Improved Cognition Activity and Minimized Neurotoxicity." *Journal of Molecular Structure* 1251: 131972. https://doi.org/10.1016/j.molstruc.2021.131972.

Aldred, K. J., R. J. Kerns, and N. Osherof. 2014. "Mechanism of Quinolone Action and Resistance." *Biochemistry* 53: 1565–1574.

Anderson, V. E., and N. Osheroff. 2001. "Type II Topoisomerases as Targets for Quinolone Antibacterials: Turning Dr. Jekyll Into Mr. Hyde." *Current Pharmaceutical Design* 7: 339–355.

Ayipo, Y. O., I. Ahmad, Y. S. Najib, S. Kehinde, H. Patel, and M. N. Mordi. 2023a. "Molecular Modelling and Structure-Activity Relationship of a Natural Derivative of o – Hydroxybenzoate as a Potent Inhibitor of Dual NSP3 and NSP12 of SARS-CoV-2: In Silico Study." *Journal of Biomolecular Structure and Dynamics* 20: 1–19. https://doi.org/10.1080/07391102.2022.2026818.

Ayipo, Y. O., W. A. Alananzeh, I. Ahmad, and H. Patel. 2023b. "Structural Modelling and In Silico Pharmacology of β-Carboline Alkaloids as Potent 5-HT1A Receptor Antagonists and Reuptake Inhibitors." *Journal of Biomolecular Structure and Dynamics* 41, no. 13: 6219–6235. https://doi.org/10.1080/07391102.2022.2104376.

Barry, A. L., W. A. Craig, H. Nadler, L. B. Reller, C. C. Sanders, and J. M. Swenson. 1999. *Methods for Determining Bactericidal Activity of Antimicrobial Agents: Approved Guideline*. National Committee for Clinical Laboratory Standards.

Bax, B. D., P. F. Chan, D. S. Eggleston, et al. 2010. "Type IIA Topoisomerase Inhibition by a New Class of Antibacterial Agents." *Nature* 466, no. 7309: 935–940. https://doi.org/10.1038/nature09197.

Bharadwaj, K. K., I. Ahmad, S. Pati, and A. Ghosh. 2022. "Potent Bioactive Compounds From Seaweed Waste to Combat Cancer Through Bioinformatics Investigation." *Frontiers in Nutrition* 9: 1–16. https://doi.org/10.3389/fnut.2022.889276.

Bisacchi, G. S. 2015. "Origins of the Quinolone Class of Antibacterials: An Expanded 'Discovery Story'." *Journal of Medicinal Chemistry* 58: 4874–4882. https://doi.org/10.1021/jm501881c.

Blondeau, J. M., R. S. M. Ccm, and S. M. Aam. 2004. "Fluoroquinolones: Mechanism of Action, Classification." *Survey of Ophthalmology* 49: 1–6. https://doi.org/10.1016/j.survophthal.2004.01.005.

Blower, T. R., B. H. Williamson, R. J. Kerns, and J. M. Berger. 2016. "Crystal Structure and Stability of Gyrase-Fluoroquinolone Cleaved Complexes From *Mycobacterium tuberculosis*." *Proceedings of the National Academy of Sciences of the United States of America* 113, no. 7: 1706–1713. https://doi.org/10.1073/pnas.1525047113.

Boulaamane, Y., I. Ahmad, H. Patel, N. Das, M. Reda, and A. Maurady. 2023. "Structural Exploration of Selected C6 and C7- Substituted Coumarin Isomers as Selective MAO-B Inhibitors." *Journal of Biomolecular Structure and Dynamics* 26: 1–15. https://doi.org/10.1080/07391102.2022.2033643.

Chuah, S., F. Tsay, P. Hsu, and D. Wu. 2011. "A New Look at Anti-*Helicobacter pylori* Therapy." *World Journal of Gastroenterology* 17, no. 35: 3971–3975. https://doi.org/10.3748/wjg.v17.i35.3971.

Demirci, A., K. G. Karayel, E. Tatar, et al. 2018. "Synthesis and Evaluation of Novel 1,3,4-Thiadiazole–Fluoroquinolone Hybrids as Antibacterial, Antituberculosis, and Anticancer Agents." *Turkish Journal of Chemistry* 42, no. 3: 839–858.

Drlica, K., H. Hiasa, R. Kerns, M. Malik, and A. Mustaev. 2009. "Quinolones: Action and Resistance Updated." *Current Topics in Medicinal Chemistry* 9: 981–998.

Farhan, M. M., M. A. Guma, M. A. Rabeea, I. Ahmad, and H. Patel. 2022. "Synthesizes, Characterization, Molecular Docking and In Vitro Bioactivity Study of New Compounds Containing Triple Beta Lactam Rings." *Journal of Molecular Structure* 1269: 133781.

Foroumadi, A., Z. Kargar, A. Sakhteman, et al. 2006. "Synthesis and Antimycobacterial Activity of Some Alkyl [5-(Nitroaryl)-1,3,4-Thiadia zol-2-Ylthio]Propionates." *Bioorganic & Medicinal Chemistry Letters* 16: 1164–1167. https://doi.org/10.1016/j.bmcl.2005.11.087.

Foroumadi, A., F. Soltani, M. H. Moshafi, and R. Ashraf-askari. 2003. "Synthesis and in v Itro Antibacterial Acti v Ity of Some N–(5-Aryl-1, 3, 4- Thiadiazole-2-Yl) Piperazinyl Quinolone Deri v Ati v Es." *Il Farmaco* 58: 1023–1028. https://doi.org/10.1016/S0014-827X(03)00191-5.

Fournier, B., X. Zhao, T. Lu, K. Drlica, D. C. Hooper, and D. C. Hooper. 2000. "Selective Targeting of Topoisomerase IV and DNA Gyrase in Staphylococcus Aureus: Different Patterns of Quinolone-Induced Inhibition of DNA Synthesis." *Antimicrobial Agents and Chemotherapy* 44, no. 8: 2160–2165.

Froelich-ammon, S. J., and N. Osheroff. 1995. "Topoisomerase Poisons: Harnessing the Dark Side of Enzyme Mechanism*." *Journal of Biological Chemistry* 270, no. 37: 21429–21432. https://doi.org/10.1074/jbc.270.37.21429.

Ghosh, S., S. Das, I. Ahmad, and H. Patel. 2021. "In Silico Validation of Anti-Viral Drugs Obtained From Marine Sources as a Potential Target Against SARS-CoV-2 M pro." *Journal of the Indian Chemical Society* 98, no. 12: 100272. https://doi.org/10.1016/j.jics.2021.100272.

Girase, R., I. Ahmad, R. Pawara, and H. Patel. 2022. "Optimizing Cardio, Hepato and Phospholipidosis Toxicity of the Bedaquiline by Chemoinformatics and Molecular Modelling Approach." *SAR and QSAR in Environmental Research* 33, no. 3: 215–236. https://doi.org/10.1080/1062936X.2022.2041724.

Heeb, S., M. P. Fletcher, S. R. Chhabra, S. P. Diggle, P. Williams, and C. Miguel. 2011. "Quinolones: From Antibiotics to Autoinducers." *FEMS Microbiology Reviews* 35, no. 2: 247–274. https://doi.org/10.1111/j.1574-6976.2010.00247.x.

Hooper, D. C. 1999. "Mode of Action of Fluoroquinolones." *Drugs* 58, no. Suppl 2: 6–10.

Hooper, D. C. 2001. "Mechanisms of Action of Antimicrobials: Focus on Fluoroquinolones." *Clinical Infectious Diseases* 32, no. Supplement_1: S9–S15. https://doi.org/10.1086/319370.

Huang, J., M. Wang, B. Wang, et al. 2016. "Bioorganic & Medicinal Chemistry Letters Synthesis, Antimycobacterial and Antibacterial Activity Derivatives Containing an Oxime Functional Moiety." *Bioorganic and Medicinal Chemistry Letters* 26: 2262–2267. https://doi.org/10.1016/j.bmcl.2016.03.050.

Jazayeri, S., M. Hassan, L. Firoozpour, and S. Emami. 2009. "Synthesis and Antibacterial Activity of Nitroaryl Thiadiazole – Gatifloxacin Hybrids." *European Journal of Medicinal Chemistry* 44, no. 3: 1205–1209. https://doi.org/10.1016/j.ejmech.2008.09.012.

Kulabaş, N., A. Türe, A. Bozdeveci, et al. 2022. "Novel Fluoroquinolones Containing 2-Arylamino-2-Oxoethyl Fragment: Design, Synthesis, Evaluation of Antibacterial and Antituberculosis Activities and Molecular Modeling Studies." *Journal of Heterocyclic Chemistry* 59, no. 5: 909–926. https://doi.org/10.1002/jhet.4430.

Lange, C., K. Dheda, D. Chesov, A. M. Mandalakas, Z. Udwadia, and C. R. J. Horsburgh. 2019. "Management of Drug-Resistant Tuberculosis." *Lancet (London, England)* 394, no. 10202: 953–966. https://doi.org/10.1016/S0140-6736(19)31882-3.

Lesher, G. Y., E. J. Froelich, M. D. Gruett, J. H. Bailey, and R. P. Brundage. 1962. "1,8-Naphthyridine Derivatives. A New Class of Chemotherapeutic Agents." *Journal of Medicinal and Pharmaceutical Chemistry* 5, no. 5: 1063–1065. https://doi.org/10.1021/jm01240a021.

Levine, C., H. Hiasa, and K. J. Marians. 1998. "DNA Gyrase and Topoisomerase IV: Biochemical Activities, Physiological Roles During Chromosome Replication, and Drug Sensitivities." *Biochimica et Biophysica Acta* 1400: 29–43.

Machado, D., E. Azzali, I. Couto, G. Costantino, M. Pieroni, and M. Viveiros. 2018. "Adjuvant Therapies Against Tuberculosis: Discovery of a 2-Aminothiazole Targeting *Mycobacterium Tuberculosis* Energetics Adjuvant Therapies." *Future Microbiology* 13, no. 12: 1383–1402. https://doi.org/10.2217/fmb-2018-0110.

Martínez-hoyos, M., E. Perez-herran, G. Gulten, et al. 2016. "EBioMedicine Antitubercular Drugs for an Old Target: GSK693 as a Promising InhA Direct Inhibitor." *EBIOM* 8: 291–301. https://doi.org/10.1016/j.ebiom.2016.05.006.

Mohammed, H. H. H., A. Ali, A. El-hafeez, S. H. Abbas, E. M. N. Abdelhafez, and G. E. A. Abuo-rahma. 2016. "New Antiproliferative 7- (4- (N -Substituted Carbamoylmethyl) Piperazin-1-Yl) Derivatives of Ciprofloxacin Induce Cell Cycle Arrest at G 2/M Phase." *Bioorganic & Medicinal Chemistry* 24, no. 19: 4636–4646. https://doi.org/10.1016/j.bmc.2016.07.070.

Nandurkar, Y., M. R. Bhoye, D. Maliwal, et al. 2023. "European Journal of Medicinal Chemistry Synthesis, Biological Screening and In Silico Studies of New Potential Antifungal and Antitubercular Agents." *European Journal of Medicinal Chemistry* 258: 115548. https://doi.org/10.1016/j.ejmech.2023.115548.

Nieto, M. J., F. L. Alovero, R. H. Manzo, and M. R. Mazzieri. 2005. "Benzenesulfonamide Analogs of Fluoroquinolones. Antibacterial Activity and QSAR Studies." *European Journal of Medicinal Chemistry* 40: 361–369. https://doi.org/10.1016/j.ejmech.2004.11.008.

Nishida, T., Y. Kuse, K. Mochizuki, M. Shimazawa, T. Yamamoto, and H. Hara. 2017. "Protective Effects of Fluoroquinolones on UV-Induced Damage of Cultured Ocular Cell Lines." *European Journal of Pharmacology* 806: 59–66. https://doi.org/10.1016/j.ejphar.2017.04.004.

Osmaniye, D., Ş. Karaca, B. Kurban, et al. 2022. "Design, Synthesis, Molecular Docking and Molecular Dynamics Studies of Novel Triazolothiadiazine Derivatives Containing Furan or Thiophene Rings as Anticancer Agents." *Bioorganic Chemistry* 122: 105709. https://doi.org/10.1016/j.bioorg.2022.105709.

Panda, S. S., S. Liaqat, A. S. Girgis, A. Samir, C. D. Hall, and A. R. Katritzky. 2015. "Bioorganic & Medicinal Chemistry Letters Novel Antibacterial Active Quinolone – Fluoroquinolone Conjugates and

2D-QSAR Studies." *Bioorganic & Medicinal Chemistry Letters* 25, no. 18: 3816–3821. https://doi.org/10.1016/j.bmcl.2015.07.077.

Pandit, N., K. Shah, N. Agrawal, N. Upmanyu, S. K. Shrivastava, and P. Mishra. 2016. "Synthesis, Characterization and Biological Evaluation of Some Novel Fluoroquinolones." *Medicinal Chemistry Research* 25, no. 5: 843–851. https://doi.org/10.1007/s00044-016-1526-x.

Paton, J. H., D. S. Reeves, M. Microbiology, and S. Hospital. 1988. "Fluoroquinolone Antibiotics." *Drugs* 36: 193–228.

Price, L. B., A. Vogler, T. Pearson, J. D. Busch, J. M. Schupp, and P. Keim. 2003. "In Vitro Selection and Characterization of *Bacillus Anthracis* Mutants With High-Level Resistance to Ciprofloxacin." *Antimicrobial Agents and Chemotherapy* 47, no. 7: 2362–2365. https://doi.org/10.1128/AAC.47.7.2362.

Radwan, H. A., I. Ahmad, I. M. M. Othman, et al. 2022. "Design, Synthesis, In Vitro Anticancer and Antimicrobial Evaluation, SAR Analysis, Molecular Docking and Dynamic Simulation of New Pyrazoles, Triazoles and Pyridazines Based Isoxazole." *Journal of Molecular Structure* 1264: 133312. https://doi.org/10.1016/j.molstruc.2022.133312.

Shaw, D. E. 2021. "Schrödinger Release 2022–2 (DE Shaw Research): Desmond Molecular Dynamics System, Maestro-Desmond Interoperability Tools."

Shirude, P. S., P. Madhavapeddi, M. Naik, et al. 2013. "Methyl-Thiazoles: A Novel Mode of Inhibition With the Potential to Develop Novel Inhibitors Targeting InhA in Mycobacterium Tuberculosis." *Journal of Medicinal and Pharmaceutical Chemistry* 56, no. 21: 8533–8542.

Sriram, D., A. Aubry, and L. M. Fisher. 2006. "Gatifloxacin Derivatives: Synthesis, Antimycobacterial Activities, and Inhibition of *Mycobacterium Tuberculosis* DNA Gyrase." *Bioorganic & Medicinal Chemistry Letters* 16: 2982–2985. https://doi.org/10.1016/j.bmcl.2006.02.065.

Talath, S., and A. K. Gadad. 2006. "Synthesis, Antibacterial and Antitubercular Activities of Some 7-[4-(5-Amino-[1,3,4]Thiadiazole-2-Sulfonyl)-Piperazin-1-Yl] Fluoroquinolonic Derivatives." *European Journal of Medicinal Chemistry* 41: 918–924. https://doi.org/10.1016/j.ejmech.2006.03.027.

Tatar, E., S. Karakus, S. G. Küçükgüzel, et al. 2016. "Design, Synthesis, and Molecular Docking Studies of a Conjugated Thiadiazole-Thiourea Scaffold as Antituberculosis Agents." *Biological and Pharmaceutical Bulletin* 39, no. 4: 502–515. https://doi.org/10.1248/bpb.b15-00698.

Tiberi, S., N. Utjesanovic, J. Galvin, et al. 2022. "Drug Resistant TB–Latest Developments in Epidemiology, Diagnostics and Management." *International Journal of Infectious Diseases* 124, no. Suppl: S20–S25. https://doi.org/10.1016/j.ijid.2022.03.026.

Türe, A., N. Kulabaş, S. İ. Dingiş, et al. 2019. "Design, Synthesis and Molecular Modeling Studies on Novel Moxifloxacin Derivatives as Potential Antibacterial and Antituberculosis Agents." *Bioorganic Chemistry* 88: 102965. https://doi.org/10.1016/j.bioorg.2019.102965.

Wayne, L. G., and L. G. Hayes. 1996. "An In Vitro Model for Sequential Study of Shiftdown of *Mycobacterium tuberculosis* Through Two Stages of Nonreplicating Persistence." *Infection and Immunity* 64, no. 6: 2062–2069. https://doi.org/10.1128/iai.64.6.2062-2069.1996.

WHO. 2024. *2024 Global Tuberculosis Report*. WHO.

Wiles, J. A., B. J. Bradbury, and M. J. Pucci. 2010. "New Quinolone Antibiotics: A Survey of the Literature From 2005 to 2010." *Expert Opinion on Therapeutic Patents* 20, no. 10: 1295–1319. https://doi.org/10.1517/13543776.2010.505922.

Zrieq, R., I. Ahmad, M. Snoussi, E. Noumi, and M. Iriti. 2021. "Tomatidine and Patchouli Alcohol as Inhibitors of SARS-CoV-2 Enzymes (3CLpro, PLpro and NSP15) by Molecular Docking and Molecular Dynamics Simulations."

Supporting Information

Additional supporting information can be found online in the Supporting Information section.